Simulating Electrohydraulic Soft Actuator Assemblies Via Reduced Order Modeling

Travis Hainsworth[1], Ingemar Schmidt[1], Vani Sundaram[1], Gregory L. Whiting[1], Christoph Keplinger[2], Robert MacCurdy[1*]

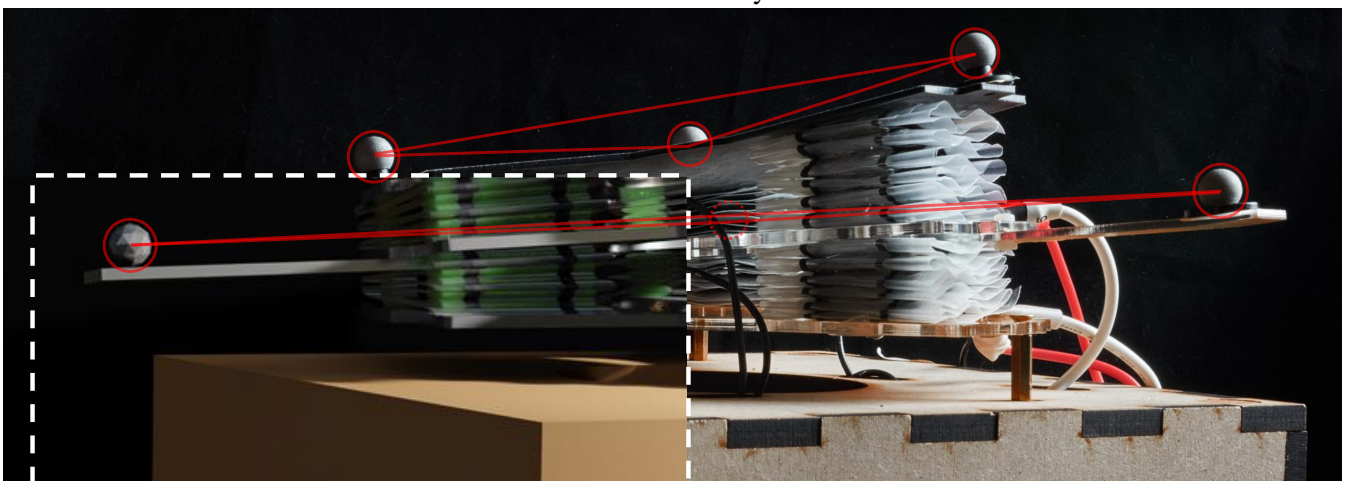

Fig. 1. Presented here is a method to simulate how an assembly of soft actuators will behave in the time domain (here the simulation is represented by the green render), and the model to do so is data driven through the use of motion capture data (solid red lines).

***Abstract*— Soft robots compliment traditional rigid robots by expanding their capabilities to interact with the physical world. A robot made with compliant, soft materials can benefit from their inherent continuum mechanics to achieve interactions with the environment that a rigid robot may find difficult. This can include grasping delicate objects, navigating through variable terrain, or working alongside humans in a safer manner. The flexible, adaptable nature of soft robots provide these benefits, but they also make predicting their actuated response a difficult, computationally-intensive task. Here we provide a non-linear, reduced order model informed by collected data on hydraulically amplified self-healing electrostatic actuators (HASELs). With this reduced order model, we simulate robots comprised of multiple actuators in an effort to rapidly evaluate potential design candidates without the need for time-consuming manufacturing. The simulation leverages a reduced-order model of HASELs based on a parallel mass spring damper (MSD) representation, made of two non-linear springs, and a damper; this data-driven parameter identification aids model fidelity. We construct a robotic manipulator actuated via six HASELs and show that the simulations driven by the non-linear MSD models accurately predict the robot's physical behavior on a macro scale. While this work focuses on a specific actuator type, the approach shown here could be extended to other linearly expanding soft actuators. Using this method, soft robotic assemblies actuated via HASELs can be rapidly evaluated in simulation before a laborious manufacturing process, which in turn will allow for faster design iterations to create more effective robots.**

This work was supported by SEMI and its FlexTech Group, a Delaware not-for-profit corporation via contract FT19-20-192

[1]Authors are with the Department of Mechanical Engineering, University of Colorado Boulder, Boulder, CO, USA

[2]Author is with a) Robotic Materials Department, Max Planck Institute for Intelligent Systems, Stuttgart, Germany b) Paul M. Rady Department of Mechanical Engineering, University of Colorado, Boulder, CO, USA c) Materials Science and Engineering Program, University of Colorado, Boulder, CO, USA

* Corresponding author maccurdy@colorado.edu

I. Introduction

Simulating and modeling the dynamics of soft actuators is a critical step toward designing effective soft robots, which as Hawkes *et. al* point out, is an open problem [1]. Micharet and Laschi discuss the recent advances in the field of modeling specifically [2]. While the progress is substantial, the works presented primarily focus on modeling of a single actuator. Beyond the analysis of a single actuator is the problem of analyzing an assembly of soft actuators as they impart forces on a robot. As Karel Capek and the root of the word imply [3], a robot should be capable of performing useful tasks and labor. In most cases a single actuator would not be sufficient to perform useful tasks, but single actuator modeling currently dominates the soft robotic research field. Being able to simulate how an entire robot will behave in various circumstances is a key component of morphological design strategies. Rigid roboticists have recognized this simulation need and have made many tools to accomplish the task; notable examples from a large field include ROS (robot operation system) and VREP (virtual robotics experiment platform, now known as Coppelia SIM). Despite the breadth of tools available to simulate traditional rigid robots, designers of soft robots typically resort to implementing their own tool-sets, specific to the robot they

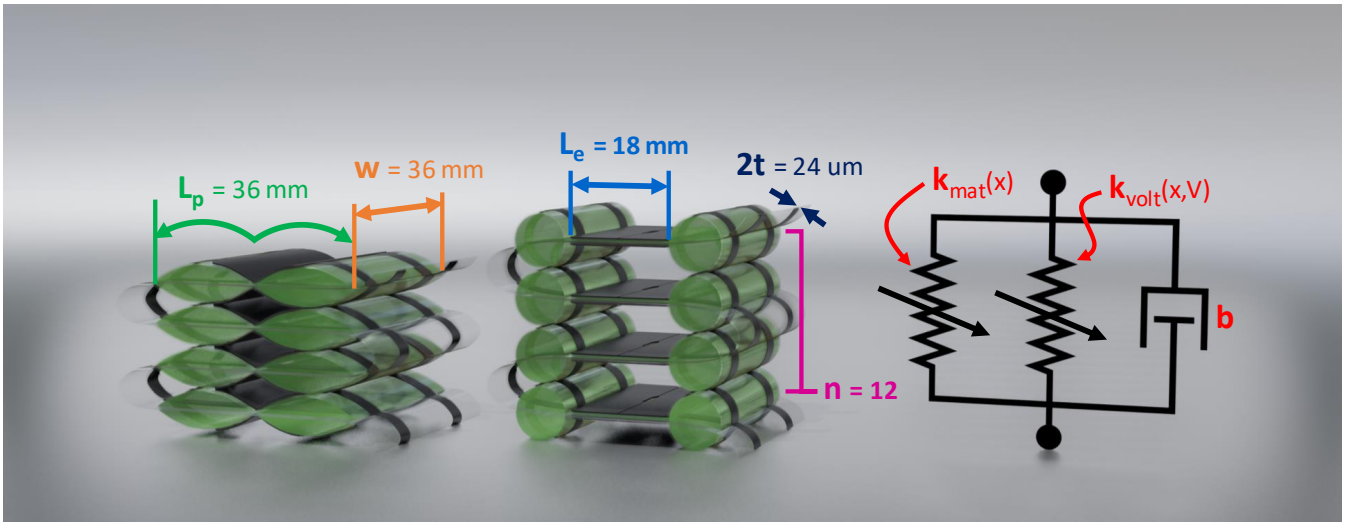

Fig. 2. The HASELs are made of individual pouches that are folded atop each other to create n layers. In this depiction $n = 4$ for visual clarity, but the HASELs used in this study have 12 layers. As electricity is applied to the actuator it goes from its resting height (left), to its maximum stroke (middle). The HASELs are reduced to two non-linear springs and a damper connected by two point masses (right)

are designing. In this paper we present a generalizable, computationally efficient method based on lumped parameter modeling to simulate a hybrid rigid-soft robot actuated by the recently developed HASEL actuators [4][5]. While this method is shown for one particular style of HASELs, this work can serve as a template for simulations of other types of linear soft actuators.

As continuum machines, soft robots present a unique challenge: there is a constant tension between simulation fidelity and speed. High-fidelity tools like SOFA [6] and its plugin for soft robotics [7] utilize continuum material models that couple material properties and distribution to macroscopic behaviors, albeit at substantial computational cost. Chain Queen [8] is another popular high-fidelity tool with a soft robotics plugin [9]. In contrast, simulation methods that prioritize speed do so through heuristics that are specific to a particular material or design morphology. Many of these come from video game development and focus on visual realism, rather than physics. These methods have been used in soft actuator applications as Rieffel *et. al* have shown, but the authors point out that attempting to incorporate real world properties in a system made for video games can be a "frustratingly cryptic system" [10].

The Keplinger Research Group has done theoretical modeling of HASELs for *contracting* "Peano"-style HASELs for both quasi-static and dynamic actuation [11][12]. Kellaris *et al.* [11] show that the maximum quasi-static stroke and force that a contracting HASEL will exhibit can be predicted based on the applied voltage, dimensions, and materials. Rothemund *et al.* [12] show how the rise and fall time of the contracting actuators can be predicted in the frequency domain, and develop a dynamical model for contractile HASELs.

Outside of HASEL modeling, various other techniques have been used to simulate soft robots. Hiller and Lipson made a simulation tool that uses Euler-Bernoulli beam theory to visualize how potential morphologies of voxels can behave together [13]. Huang *et al.* use symplectic Newmark-beta time integration to model how elastic rods will behave in different morphologies, and they verify their simulations with shape memory alloy (SMA) actuators [14]. Duriez *et al.* use the simulation framework SOFA [6] to model pneumatic and cable driven actuators. They use continuum mechanics to model the material's internal forces, Signorini's law for contact, and Lagrangian multipliers for constraints [15]. Martin-Barrio *et al.* created a 1.2 m long cable-driven tentacle-like robot which they modeled using FEM via the Soft Robotics plugin to SOFA to allow real-time control up to 20 Hz [16]. Johnson *et al.* use linear frequency response tests to characterize the dynamics of folded HASELs. This work treated the activation (increased input voltage) and relaxation (decreased input voltage) responses as two separate dynamic modes to simplify the nonlinear system dynamics [17]. Maffli *et al.* created a model of electrostatic zipping to predict the dynamics of DEAs [18]. Zui *et al.* used VOXCAD [13] to simulate and evolve the gaits of pressure actuated, modular soft cubes [19].

Rather than develop a complete multi-physics simulation of a HASEL, which would be computationally intractable to use with a practical robot, or resort to design-specific heuristics, we develop a reduced order model of a HASEL, with parameters that are determined by experimental data. Here we aim for a balanced simulation that favors speed, while representing the essential dynamics of a structure actuated via HASELs. As such, the method developed in this paper can be used to simulate arbitrary robot morphologies that employ HASEL actuators. The actuators used in this paper are linearly *expanding*, electrostatic foldable HASEL actuators [4][20]. We chose to represent these actuators with a nonlinear Mass Spring Damper model (MSD). Zhang explicitly points out that an MSD model with general Hookean

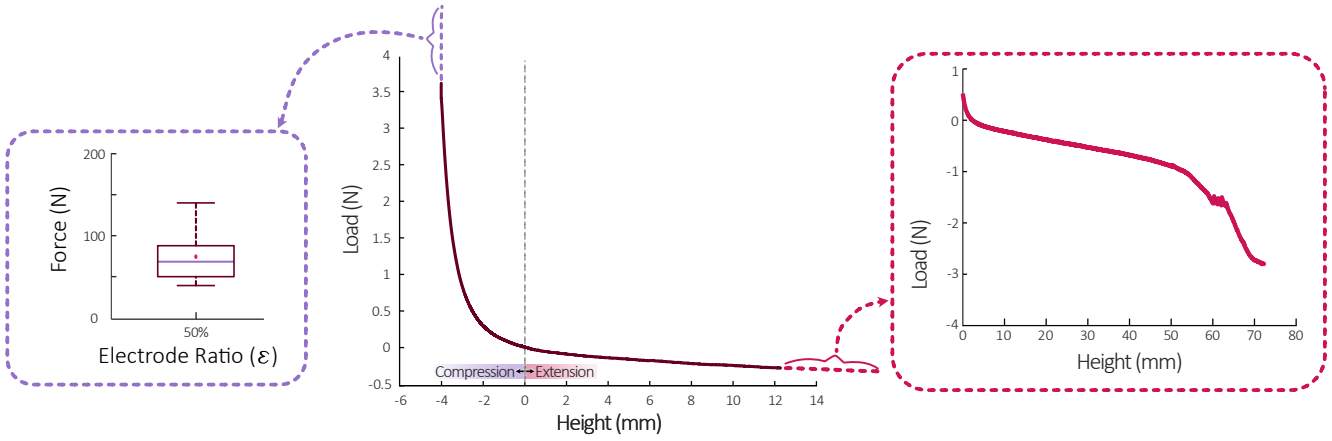

Fig. 3. To determine the bounds of the HASEL's strength, we compressed 10 actuators until they ruptured (left plot), giving a metric for the compressive strength of an actuator. On the opposite end (right plot), we pulled 36 actuators apart in tension to measure the strength of interlayer adhesion. Using a reduced value of these limits, we subjected each actuator to compressive and tensile cyclic loading at various applied voltages, and this test at 0 kV is shown in the center plot (mean of $n = 4$). Each voltage results in an independent curve, and later we compile these curves into various surfaces.

springs has a big O complexity lower than Finite Element Analysis, the energy minimization method, and the rigid-body deformation method [21], while Wang *et al.* also discuss the need for accurate models of nonlinear soft robotic actuators [22]. In contrast to previous work, we aim to simulate assemblies of actuators, not just a single actuator, which can be used to inform physical design and control decisions. To support this effort, we not only present simulation results, but also include a comparison to a physical robot. Additionally, rather than using simulation constants that lack physical meaning, as is common in video game simulations, we use experimental data to develop the MSD's force vs displacement properties. While we use measurements in this paper, constitutive models similar to those presented in [12] would also be compatible with our simulation approach.

In summary, we present:

- A non-linear reduced-order MSD model of a HASEL actuator
- Data for determining the model's parameters
- Details on manufacturing the physical actuators from which the data is derived
- An approach to efficiently simulate the dynamics of assemblies of HASEL actuators using the MSD model

II. Methods

A few key considerations should be considered when endeavoring to simulate a robotic assembly. For example, how quickly must the simulation run? In this work, we are creating a method to simulate robotic assemblies, rather than individual actuators, with the goal of quickly iterating through potential designs, and while we are prioritizing speed over accuracy, we still want accuracy on the macro scale of the robot. With that goal we decided on a simulation compilation time of < 5 minutes with accuracy of < 5 mm as our constraints. Given these constraints, what model should we use? A mass-spring-damper (MSD) model of an actuator, with proper parameters, will fulfill our constraints and provides a natural way to assemble many different actuators into robotic assembly design candidates, even if they have different parameters. Given this model choice, what parameters must be characterized? For an MSD model, spring and damper coefficients must be chosen to predict an actuator's behavior in the time domain, with varying loads and applied voltages. However, HASELs exhibit highly nonlinear behavior both in the quasi-static and dynamic regime [12]. Furthermore, HASELs are not passive nonlinear springs; they are voltage-actuated devices with force vs position characteristics that depend on the applied voltage. Therefore, the numeric spring coefficients lie on a nonlinear surface which is dependent on both voltage and position, in contrast to the traditional, single constant used in Hookean spring models. In this section we detail this process by a) describing the design parameters for manufacturing the HASELs, b) elucidating the data acquisition methodology reported in Section III, c) explaining how we reduced the data into a MSD model, d) outlining the steps required to simulate HASELs, and e) describing the robotic assembly that we used for validation of our model choice.

A. Actuator Design and Fabrication

Our HASEL manufacturing methods are largely adopted from Mitchel *et al.* [20], and are made of two heat-sealable layers of 12 μm thick PET (*Mylar 850H*, dielectric constant of 3.1), to encapsulate the FR3 dielectric fluid (*Cargill*, density of 0.92 g/cm^2, dielectric constant of 3.2). The two sheets of Mylar are heat-sealed together using a CNC machine with a modified head (*Shapeoko 3XL, Carbide 3D*). A layer of conductive, carbon-based ink (*EMS CI-2051*) is screen printed on the outer sides of the Mylar shell (see the black planes in Figure 2) to create the actuator's electrodes; one electrode connects to the ground plane, and the other connects to a high voltage source. The individual layers of the HASEL consist of two discrete, parallel pouches that are each partially covered by the electrodes, Figure 2 outlines the dimensions of the pouch and electrodes. Each of those

pouches is filled with dielectric fluid and the amount of fluid is optimized and determined by:

$$V = \frac{(L_p * (1 - f_e))^2 * w}{2 * \pi} \quad (1)$$

where L_p is the length of the pouch, and w is the width of the pouch, as depicted in Figure 2 [11]. The ratio of electrode coverage to pouch length (f_e) is:

$$f_e = \frac{L_e}{L_p} = 50\% \quad (2)$$

where L_e is the length of the electrode, as seen in Figure 2.

B. Data Collection

We performed a quasi-static analysis to obtain the force-strain curve at different applied voltages. To ensure that we did not push all of our HASELs to failure during testing (i.e. leaking, rupturing, or delaminating from neighboring layers), we determined the maximum compression and extension limits using two different tests: the first test destructively compressed a single layer until rupture occurred (Algorithm 1), and the second test extended the complete actuators until the inter-layer bonds delaminated/separated. With those limits in mind, and understanding that HASELs exhibit non-linear behavior, we measured the resulting load from a quasi-statically depressed HASEL at a fixed compression rate and at various constant input voltages (Algorithm 2).

Algorithm 1: Maximum Allowable Pressure

```
DMA in displacement control;
No applied voltage to HASEL;
DMA plate resting on HASEL (h = h_0);
while h > 0 do
    Compress HASEL (h = h − 0.1mm);
    Measure reaction force;
end
```

We found the maximum allowable compressive force and failure mode for our HASEL actuators by destructive, compressive testing. We observed that the failure mechanism was most commonly at a corner of the pouch's heat seal. This was done using a dynamic mechanical analyzer (DMA) (*TestResources*) to slowly apply incremental displacement at 0.05 mm/s to the pouch while measuring the resultant force. We ran 12 tests, obtained the force-displacement curve, and recorded the peak force before the first point of failure (see Figure 3), which will be discussed in Section III. Using a safety factor of 2, we will use half of this value for the peak applied load in the subsequent cyclic compression tests.

The next test for implementinmg our model is determining the maximum extension that a HASEL can withstand. This finishes the characterization of the HASEL's physical limits, by measuring how much tensile force the actuators can sustain along the axis of actuation. A single actuator is comprised of two pouches stacked into multiple layers (refer back to Figure 2). Each of these layers is adhered to the other

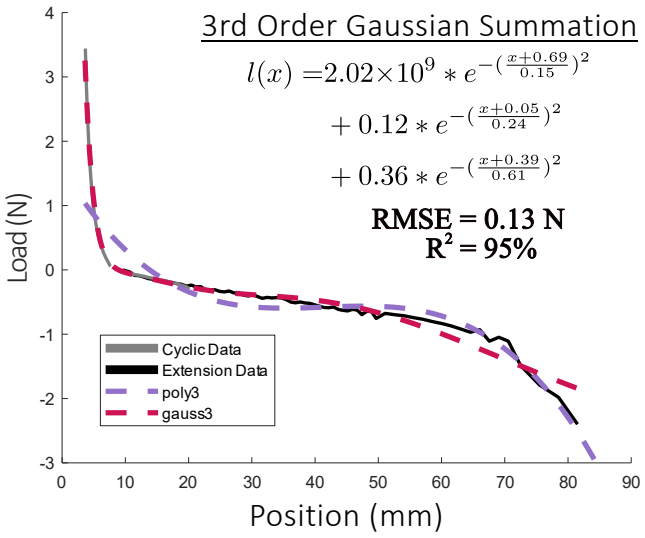

Fig. 4. To discretize a HASEL's material properties and the effects of applied voltage under compression or extension, we measured the resultant load while the HASEL was cyclically loaded with no voltage. With this data we can fit a function to represent the material response alone. ($n = 4$)

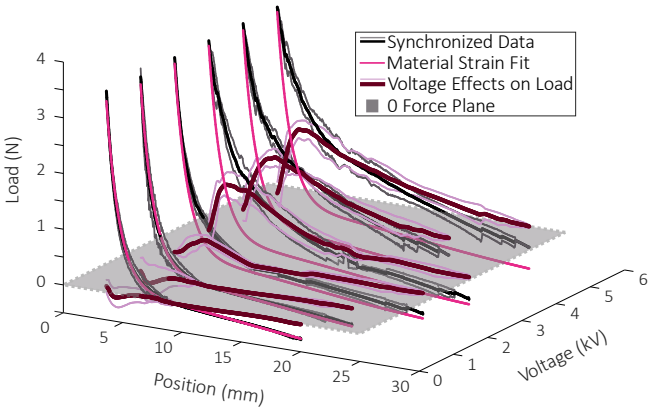

Fig. 5. We can remove the effects from material strain by subtracting its fit (Figure 4 and the pink curves here). In doing so, we are left with the effects of voltage alone. This data was taken at 1 kHZ over 3 minutes and both the "Voltage Effects on Load" and "Data" curves highlight the 95% confidence intervals.

with a strip of 3M Permanent Double-Sided tape that is 14 mm wide by 1.5 mm long. In all cases this will be the failure point in extension; the tape securing the layers together will detach before a heat seal is broken. So, we determine how much force will cause delamination of two pieces of Mylar sandwiched together with the tape.

To find the maximum sustained tensile force, each HASEL sample was bonded to flat plates via the same 3M tape, which were then fixed to the DMA's specimen fastening points. The tape connecting the HASELs to the plates was applied in excess, to assure that the point of failure would be between two consecutive HASEL layers, rather than between HASEL and plate. The HASELs were then gradually stretched at a rate of 2 mm/s until a tape bond failed. The results of this test are shown in the right side of Figure 3.

After gathering the data to characterize the material me-

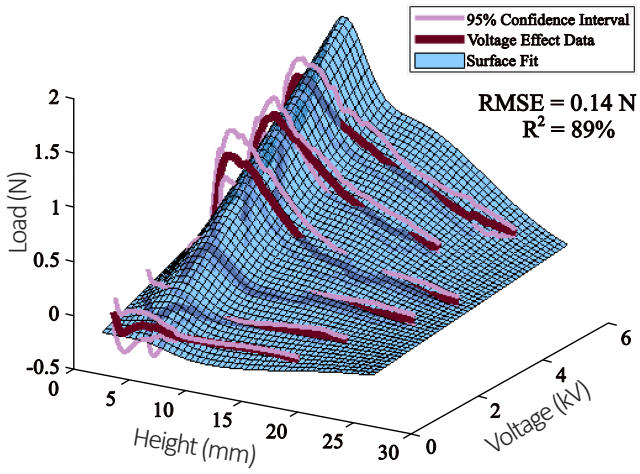

Fig. 6. With data that has material strain effects removed, we can fit a surface that predicts how the HASEL will respond to applied voltages alone. This surface fit is a 3rd order Gaussian Exponential based on height, but the amplitude of each exponential is a 1st degree polynomial based on voltage (Equation 10).

chanics of the actuator, we gathered data that characterizes the actuation when voltage is applied to the HASEL. We achieve this by obtaining the force vs. position curve under quasi-static loading at various applied voltages supplied by a TREK 610E. To do this we use the DMA to slowly apply a load at a constant rate of 0.75 mm/s to an actuated HASEL, as outlined in Algorithm 2. The results are shown in Figure 5, and are explored further in Section III.

Algorithm 2: Quasi-Static HASEL Compression at Varying Voltages

```
DMA in displacement control;
No applied voltage to HASEL (v = 0);
DMA plate resting on HASEL (h = h_0);
while v < v_max + 1 do
    while force > ruptureforce/2 do
        Compress HASEL (h = h − 0.1mm);
        Measure reaction force;
    end
    Move DMA to top position (no HASEL contact);
    Increase voltage (v + +);
end
```

In order to validate our assumption that the dynamics of the actuated assembly composed of multiple HASELs are slower than the individual dynamics of a single actuator, we measure the time response to an actuator subjected to various voltage step inputs (1, 2, 3, 4, and 5 kV) with no external force applied, as outlined in Algorithm 3. This test was done with a Keyence LK-H157 laser displacement sensor.

C. Model Reduction

We derive our model from Newton's Second Law:

$$m\ddot{\mathbf{x}} = \mathbf{f_i} + \mathbf{f_b} + \mathbf{f_s} \tag{3}$$

Algorithm 3: Dynamic Analysis of No Force Load Response at Varying Voltages

```
Adhere a thin card to a single pouch of the top layer
  for laser accuracy;
while v < v_max do
    Apply a step input (v);
    Measure the displacement of the actuator until
      steady state is achieved;
    Turn off the voltage;
    Allow at least 10 s for accumulated charge to
      dissipate;
end
```

where $\mathbf{f_i}$ are internal forces, $\mathbf{f_b}$ are body forces, such as gravity, and $\mathbf{f_s}$ are surface forces, such as external disturbances. For our reduction we will treat $\mathbf{f_i}$ as a mass spring damper system:

$$\mathbf{f_i} = k_{material}(\mathbf{x})\mathbf{x} + k_{voltage}(\mathbf{x}, V)\mathbf{x} + b\dot{\mathbf{x}} + \tau\theta \tag{4}$$

where $\mathbf{x}$ is the vector displacement of the actuator from rest, V is the applied voltage, θ is the angular displacement from rest, and τ is the corresponding restoration constant ($\tau\theta$ is a Hookean model of a torsional spring). Once the quasi-static force vs displacement curve (Figure 3) has been obtained, we identify a curve that represents the restoring force of the actuator's material properties by solving equation 3 after the system has come to rest and no voltage is applied ($V = 0kV$). While no voltage is applied $k_{voltage}(x, V) = 0$, so equation 4 simplifies to:

$$\mathbf{f_i} = k\mathbf{x} + b\dot{\mathbf{x}} + \tau\theta \tag{5}$$

then substituted into equation 3:

$$m\ddot{\mathbf{x}} = k\mathbf{x} + b\dot{\mathbf{x}} + \tau\theta + \mathbf{f_b} + \mathbf{f_s} \tag{6}$$

then simplified based on the quasi-static nature of the test:

$$0 = k\mathbf{x} + 0 + 0 + \mathbf{g} + \mathbf{f_s} \tag{7}$$

where

Once an MSD model of the HASEL has been determined we use it to simulate larger assemblies of HASELs which can make up a robot, or part of a robot. In the simulation, the MSD models of each HASEL are attached to each other with rigid links as-dictated by the design to create the larger morphology (for example, the Stewart platform shown in Figure 8). These attachments create the full equations of motion, which are captured in an automatically-generated design-specific 1st order ODE file. Then the system is numerically integrated in the time domain using MATLAB's ODE45. Throughout this time integration, different actuators can be turned on and off, and the whole system will respond accordingly. The simulation also accounts for gravity and external forces by adding those forces to each of the coupled MSD equations.

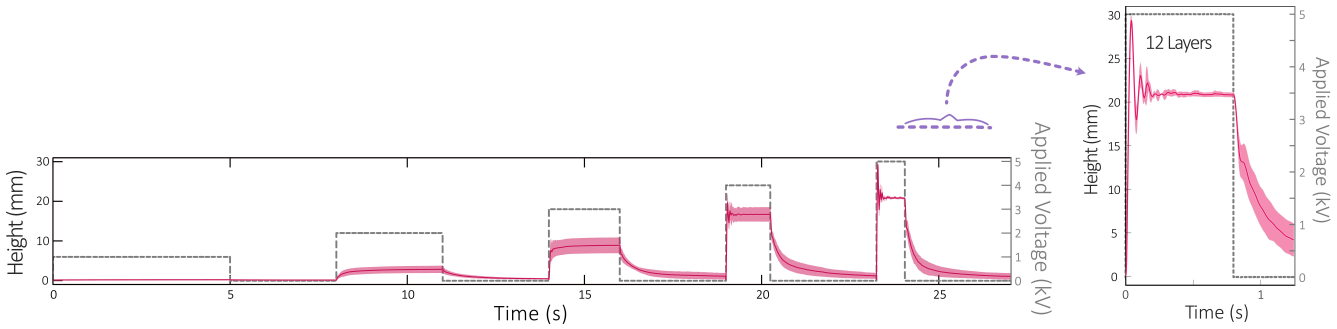

Fig. 7. Measuring the dynamic response to applied voltage shows first-order transient behavior. Across all applied voltages, rise times are significantly shorter than the time scales of interest for assembled robot simulations, motivating our choice to neglect any time dependent terms in our model for actuation force. ($n = 4$ with a shaded 95% confidence interval)

D. Verification

We created a simplified two-stage Stewart platform, seen in Figure 8, to verify the fidelity of our model. Each stage supports three actuators and is designed for interchangeable actuators. We applied input voltages to each of the platform's six actuators ranging from 0-5kV using a high voltage amplifier (*610E, TREK*). We used a four-camera motion capture system (*OptiTrack*) to track the changes in actuator height and the platform's end effector. The predicted movement of the platform simulated in the time domain was compared to the motion capture data, which we treated as ground truth.

III. Results

A. HASEL Characterization

Compression of a single layer until failure produces an interesting two-peak response that arises from the discrete failure of each of the two pouches that make up each layer. Dimensional variations, inevitable in manufacturing, result in different critical displacement distances required to rupture each pouch. One might be tempted to use the peak force as the strength of the layer, or perhaps even average the two, but any rupture would be a failure, and for that reason we only look at the first (lowest) peak. We compressed a single layer of the HASEL at 0.05 mm/s until a displacement of 0.2*resting height, that guaranteed rupture of both pouches. We repeated this test five times, each on a new sample, to obtain the results on the left side of Figure 3. Using this data, we chose to cyclically compress the HASELs to 4.4 N (providing a factor of safety of roughly 2) and use that for both springs' characterization.

For the maximum extension we found that a Mylar-double sided tape sandwich can withstand 4.3 N of extending force. We used the data from this test, in tandem with the cyclic compression test at 0 kV, to characterize the material strain model ($k_{material}(x)$ in equation 4).

The rise time of HASELs is quite short, about 0.017s, as shown in Figure 7. We use this short rise time contrasted with the simulation durations to justify the use of a single b constant.

B. Model Generation

To characterize the material properties of the actuator, we experimented with 13 different fit types. Two of these fit types are highlighted in Figure 4, overlaid atop the combined cyclic compression and peel test data. The 3rd order Gaussian exponential fits the compression side of the data, while the 3rd order polynomial more closely fits the extension side of the data. These actuators are designed to operate in compression, but they are not designed to resist tension, so with this in mind, we favored the closer fit of the compression data that the 3rd order Gaussian exponential provided. The resultant fit takes the form of:

$$\begin{aligned} l_{material}(x) = 2.02 \times 10^9 * e^{-(\frac{x+0.69}{0.15})^2} \\ +0.12 * e^{-(\frac{x+0.05}{0.24})^2} \\ +0.36 * e^{-(\frac{x+0.39}{0.61})^2} \end{aligned} \tag{8}$$

which predicts the restoring force to within a 0.13 N deviation (root mean squared error), and the fit can explain 95% of the effects due to 0 kV loading data (root squared error). This can then be arranged to take the form of a spring:

$$k_{material} = l_{material}(x)/x \tag{9}$$

The fit of the material data is then subtracted from the cyclic compression data at higher voltages as shown in Figure 5. This new data set represents any properties not related to the material strain, which in these actuators should be dominated by the effects of applying voltage to the system. This assumption is supported by the relatively low force magnitude at 0 kV, and the increasing response at higher voltages. We observe experimentally that with no applied load, visible actuation doesn't occur until $\sim$ 2 kV, and it isn't until $\sim$ 3 kV that large displacements are noticeable. Figure 6 shows the final surface that represents the data. This surface is a 3rd order Gaussian exponential with respect to displacement, and a 1st order polynomial with respect to voltage:

$$\begin{aligned} l_{volt}(x, V) =& (0.49 * V + 0.04) * e^{(\frac{x-0.11}{0.11})^2} + \\ & (0.66 * V - 0.14) * e^{-(\frac{x-0.31}{0.43})^2} - \\ & (1.80 * V + 4.60) * e^{(\frac{x-2.5}{0.2})^2} \end{aligned} \tag{10}$$

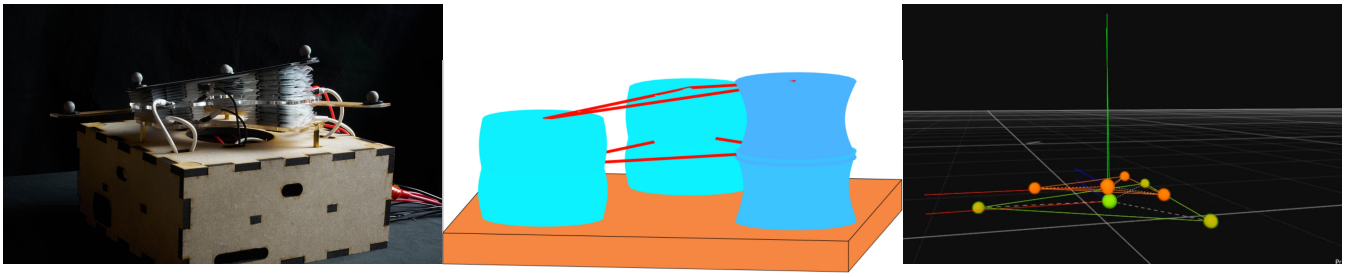

Fig. 8. To verify our simulation models (center) we constructed a 2 stage robot modeled after Stewart platform (left), and while the robot's end effector was active it was tracked with a motion capture system (right).

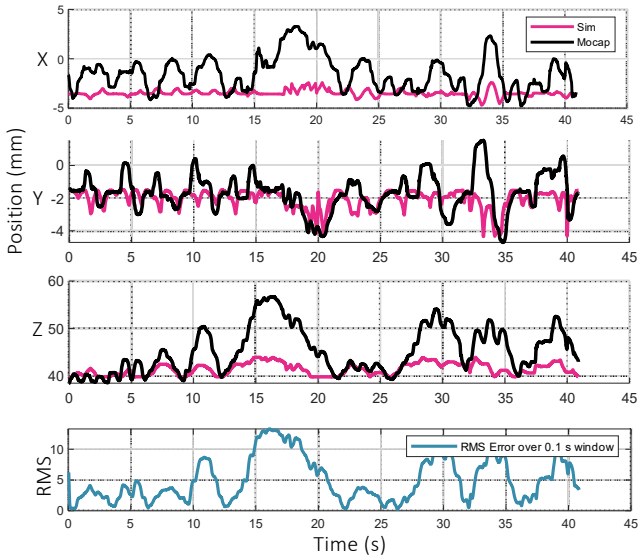

Fig. 9. Comparing the distance of the simulated and motion captured end effectors (the center of the top platform). The simulation tracks the profile that the motion capture system recorded, the error varies, but the total RMS error throughout the simulation is 6.24 mm, 25% above the stated goal of 5 mm. See the supplementary video for the real time demonstration comparing the simulation to the platform.

which has a RMSE of 0.14 N and a R^2 residual of 89%.

Because we are presently focused on the low-frequency response of the system, we choose a damping coefficient by visual estimation, with simulation speed as a priority. We tuned the damping coefficient, b of equation 6, so that the simulator runs quickly while maintaining stability. In doing so, we find the constant:

$$b = 1\frac{kg}{s} \tag{11}$$

and with a similar method and arguments stated in the methods section, we find that

$$\tau = 1\frac{kg * m}{s^2} \tag{12}$$

C. Simulation Accuracy

To quantify the efficacy of the simulation, we manufactured a two-stage robot inspired by serially connected Stewart platforms as shown in Figure 8. We simulate this robot with the method described, using the presented curve and surface fits to represent the actuator behavior. The simulation can be seen in the supplemental video. To quantify the accuracy the root mean squared error was calculated using the Euclidian norm between the physical reference point and its equivalent simulation reference point (the center of the top platform) over a 0.1 s sliding time window, as shown in Figure 9. The total RMS error throughout the entire simulation is 6.24 mm, which is 25% above the stated goal of 5 mm. We don't use the R^2 error as a metric, because with the simulation taking place in the time domain the mean of the positions is meaningless, but the difference of the positions at each time (which is what we care about) would be zero in the world of a perfect simulation. This simulation has a variety of voltage inputs which includes individual actuation, multiple actuations in a defined pattern, and a random distribution of actuations. A brief video of the simulation and accompanying robot can be found in the supplementary information.

IV. Conclusion

To follow up this work, we will apply these methods to various configurations of HASELs; we will vary the electrode ratio and the number of layers for these experiments. In doing so, the relationship of how these parameters affect the curve and surface fits of the actuators can be explored. One would expect that the number of layers wouldn't change the force outputs, but that they would have a linear relationship to the stroke of the actuators. Conversely one would expect an inverse relationship of stroke and the electrode ratio, but a directly proportional relationship with the maximum force output. By repeating the methods presented here we will explore potential relationships between these parameters that could be modeled.

The work presented here gives a tutorial on how the data from cyclically loading a linearly expanding soft actuator can be used to make a simulation of potential robots in the time domain. We have shown that, in the case of quasi-static applications, these simulations can give macro-scale predictions about how HASEL actuators arranged in various configurations will behave. This work and tutorial can be used to inform roboticists on the potential viability of a design without needing to laboriously manufacture each candidate.

This material is based on research sponsored by Army Research Laboratory under Cooperative Agreement Number

W911NF-19-2-0345. The views and conclusions contained in this document are those of the authors and should not be interpreted as representing the official policies, either expressed or implied, of the Army Research Laboratory or the U.S. Government. The U.S. Government is authorized to reproduce and distribute reprints for Government purposes notwithstanding any copyright notation thereon.

C.K. acknowledges funding by the Max Planck Society, Germany

CK is listed as inventor on multiple patents and patent applications which cover fundamentals and basic designs of HASEL actuators. CK is also a co-founder of Artimus Robotics, a start-up company commercializing HASEL actuators.

References

[1] Elliot W. Hawkes, Carmel Majidi, and Michael T. Tolley. "Hard questions for soft robotics". In: *Science Robotics* 6.53 (Apr. 28, 2021), eabg6049.

[2] Concepción Alicia Monje Micharet and Cecilia Laschi. "Editorial: Advances in Modeling and Control of Soft Robots". In: *Frontiers in Robotics and AI* 8 (2021), p. 147.

[3] The Editors of Encyclopaedia Britannica. *R.U.R. play by Čapek*. Nov. 20, 2014.

[4] E. Acome et al. "Hydraulically amplified self-healing electrostatic actuators with muscle-like performance". In: *Science* 359.6371 (Jan. 5, 2018), pp. 61–65.

[5] Philipp Rothemund et al. "HASEL Artificial Muscles for a New Generation of Lifelike Robots—Recent Progress and Future Opportunities". In: *Advanced Materials* 33.19 (2021), p. 2003375.

[6] François Faure et al. "SOFA: A Multi-Model Framework for Interactive Physical Simulation". In: *Soft Tissue Biomechanical Modeling for Computer Assisted Surgery*. Ed. by Yohan Payan. Vol. 11. Studies in Mechanobiology, Tissue Engineering and Biomaterials. Springer, June 2012, pp. 283–321.

[7] Eulalie Coevoet et al. "Software toolkit for modeling, simulation and control of soft robots". In: *Advanced Robotics* 31 (Nov. 2017). Publisher: Taylor & Francis, pp. 1208–1224.

[8] Yuanming Hu et al. "ChainQueen: A Real-Time Differentiable Physical Simulator for Soft Robotics". In: *2019 International Conference on Robotics and Automation (ICRA)*. 2019 International Conference on Robotics and Automation (ICRA). Montreal, QC, Canada: IEEE, May 2019, pp. 6265–6271.

[9] Andrew Spielberg et al. "Advanced soft robot modeling in ChainQueen". In: *Robotica* (), pp. 1–31.

[10] John Rieffel et al. "Evolving soft robotic locomotion in PhysX". In: *Proceedings of the 11th Annual Conference Companion on Genetic and Evolutionary Computation Conference: Late Breaking Papers*. GECCO '09. New York, NY, USA: Association for Computing Machinery, July 8, 2009, pp. 2499–2504.

[11] Nicholas Kellaris et al. "An analytical model for the design of Peano-HASEL actuators with drastically improved performance". In: *Extreme Mechanics Letters* 29 (May 1, 2019), p. 100449.

[12] Philipp Rothemund, Sophie Kirkman, and Christoph Keplinger. "Dynamics of electrohydraulic soft actuators". In: *Proceedings of the National Academy of Sciences* 117.28 (July 14, 2020). Publisher: National Academy of Sciences Section: Physical Sciences, pp. 16207–16213.

[13] Jonathan Hiller and Hod Lipson. "Dynamic Simulation of Soft Multimaterial 3D-Printed Objects". In: *Soft Robotics* 1.1 (Mar. 2014), pp. 88–101.

[14] Weicheng Huang et al. "Dynamic simulation of articulated soft robots". In: *Nature Communications* 11.1 (Dec. 2020), p. 2233.

[15] C. Duriez et al. "Framework for online simulation of soft robots with optimization-based inverse model". In: *2016 IEEE International Conference on Simulation, Modeling, and Programming for Autonomous Robots (SIMPAR)*. 2016 IEEE International Conference on Simulation, Modeling, and Programming for Autonomous Robots (SIMPAR). Dec. 2016, pp. 111–118.

[16] A. Martin-Barrio et al. "Modelling the Soft Robot Kyma Based on Real-Time Finite Element Method". In: *Computer Graphics Forum* 39.6 (2020), pp. 289–302.

[17] Brian K. Johnson et al. "Identification and Control of a Nonlinear Soft Actuator and Sensor System". In: *IEEE Robotics and Automation Letters* 5.3 (July 2020). Conference Name: IEEE Robotics and Automation Letters, pp. 3783–3790.

[18] L Maffli, S Rosset, and H R Shea. "Zipping dielectric elastomer actuators: characterization, design and modeling". In: *Smart Materials and Structures* 22.10 (Oct. 1, 2013), p. 104013.

[19] Xin Sui et al. "Automatic Generation of Locomotion Patterns for Soft Modular Reconfigurable Robots". In: *Applied Sciences* 10.1 (Jan. 2020). Number: 1 Publisher: Multidisciplinary Digital Publishing Institute, p. 294.

[20] Shane K. Mitchell et al. "An Easy-to-Implement Toolkit to Create Versatile and High-Performance HASEL Actuators for Untethered Soft Robots". In: *Advanced Science* 6.14 (2019), p. 1900178.

[21] Zhou Zhang. "Soft-Body Simulation With CUDA Based on Mass-Spring Model and Verlet Integration Scheme". In: (2020), p. 8.

[22] Hongbo Wang, Massimo Totaro, and Lucia Beccai. "Toward Perceptive Soft Robots: Progress and Challenges". In: *Advanced Science* 5.9 (July 13, 2018).